Journal of Applied Polymer Science

Friction and Wear Properties of Graphene Oxide/Ultrahigh-Molecular-Weight Polyethylene Composites Under the Lubrication of Deionized Water and Normal Saline Solution

Yingfei An,[1,2] Zhixin Tai,[1] Yuanyuan Qi,[1,2] Xingbin Yan,[1] Bin Liu,[2] Qunji Xue,[1] Jinying Pei[3]

[1]State Key Laboratory of Solid Lubrication, Lanzhou Institute of Chemical Physics, Chinese Academy of Sciences, Lanzhou 730000, China

[2]School of Stomatology, Lanzhou University, Lanzhou 730000, China

[3]School of Stomatology, Fourth Military Medical University, Xi'an 710032, China

Correspondence to: X. Yan (E-mail: xbyan@licp.cas.cn) or B. Liu (E-mail: liubkq@lzu.edu.cn)

ABSTRACT: Ultrahigh-molecular-weight polyethylene (UHMWPE) and UHMWPE composites reinforced with graphene oxide (GO) were successfully fabricated through a new step of liquid-phase ultrasonic dispersion, high-speed ball-mill mixing, and hot-pressing molding technology. When the GO/UHMWPE composites were lubricated with deionized water (DW) and normal saline (NS) solution, their friction and wear properties were investigated through sliding against ZrO_2. The worn surface and wear volume losses of these composites were studied with scanning electron microscopy, X-ray photoelectron spectroscopy, and a Micro-XAM 3D non-contact surface profiler. The results show that the microhardness of the GO/UHMWPE composites was improved by 13.80% and the wear rates were decreased by 19.86 and 21.13%, whereas the depths of the scratches were decreased by 22.93 and 23.77% in DW and NS lubricating conditions, respectively. © 2013 Wiley Periodicals, Inc. J. Appl. Polym. Sci. **2014**, *131*, 39640.

KEYWORDS: biomedical applications; composites; friction; wear and lubrication

Received 21 January 2013; accepted 10 June 2013
DOI: 10.1002/app.39640

INTRODUCTION

Although various material combinations are used in artificial joint prostheses, ultrahigh-molecular-weight polyethylene (UHMWPE) is still the most commonly used material because of its excellent mechanical properties, including its low coefficient of friction (COF), good biocompatibility, and stability.[1–4] However, studies have demonstrated that wear is a major problem, and with increasing service years, aseptic loosening as a result of the wear debris of UHMWPE becomes one of the most important factors in the failure of joint replacement, especially in prolonged application.[5,6] Therefore, the improvement of the mechanical properties and wear resistance of pure UHMWPE is highly significant. Therefore, studies of the friction and wear properties of UHMWPE to reduce the wear debris, including the use of inorganic fillers[7–13] and carbon nanometer materials, among others,[14–19] have been carried out. However, all of these composite materials suffer from relatively high additive amounts, high costs, and unsatisfactory performance; these will limit their applications as artificial joint prosthetic materials in the future.

In our earlier study,[20] graphene oxide (GO) was used to improve the wear resistance of UHMWPE, and GO/UHMWPE composites were successfully fabricated through optimized toluene-assisted mixing, which was followed by hot pressing. The friction and wear properties of the composites were investigated under dry conditions with a reciprocating friction testing machine. The results show that when the GO content reached 1.0 wt % (the weight percentage based on UHMWPE), the wear resistance of the composites significantly improved, and the COF slightly increased. However, legalizing the production of this synthetic method is difficult because of the strong toxicities and potential dangers of toluene to human health and the environment.[21–23] Furthermore, a number of evident differences between artificial and physiological hip and knee joints have been found. Artificial joints generally consist of an UHMWPE or a ceramic acetabular cup and a metal or ceramic femoral head.[23–26] In contrast, the typical structure of the physiological joint in the human body is not only composed of an acetabulum, a femoral head, and a joint capsule, but also physiological synovial fluid, which is a type of body fluid that contains many types of water, normal saline (NS) solution, electrolytes, and biological macromolecules, among others.[27,28] In addition, the water and NS solution, in particular, are the most fundamental components of the physiological synovial fluid and are believed

to have different effects on the friction and wear behavior of the joint prosthesis material.[29,30] Xiong and Ge[28] investigated the friction and wear properties of UHMWPE sliding against Al_2O_3 ceramic in different lubricating conditions of distilled water and normal physiological saline solution. They found that the material was very sensitive in its water absorption state, and the wear mechanisms were different in dry friction conditions. A significant amount of debris was produced by the worn surface of UHMWPE in dry sliding because of microadhesive wear. However, in distilled water and normal physiological saline solution lubricating conditions, the predominant wear mechanisms were fatigue and abrasion, respectively. The wear rate (WR) in distilled water was lower than that in normal physiological saline solution. However, Cho et al.[29] reported that the COF and WR in distilled water were higher than those in NS, but the difference was not significant. Hence, the wear test should be examined in the laboratory and lubricated in water and NS solution to acquire a better understanding of the friction and wear properties of GO/UHMWPE composite materials.

Therefore, the exploration of a safe and convenient synthesis route for GO/UHMWPE composites and the acquisition of more understanding of the friction and wear behaviors in the lubricating conditions, such as in water and NS solution are significant. Therefore, in this study, to explore the potential application of GO/UHMWPE composites as a material in the field of artificial joint and industrial bearing materials, UHMWPE and UHMWPE composites reinforced with GO were successfully fabricated through a new step of liquid-phase ultrasonic dispersion, high-speed ball-mill mixing, and hot-pressing molding technology. Under the lubrication conditions of deionized water (DW) and NS solution, the friction and wear properties of the GO/UHMWPE composites sliding against ZrO_2 ceramic balls were investigated in the joint simulator of an improved tribometer apparatus.

EXPERIMENTAL

Materials

Powdered UHMWPE (M-II), with a number-average molecular weight of 2.5×10^6 g/mol and a mean particle diameter of 281.6 ± 52.3 μm (measured by a Microtrac S3500, Microtrac, Inc., Pennsylvania), was supplied by the Beijing Oriental Petrochemical Co., Ltd. (China). Analytically pure ethanol was purchased from Tianjin Reagent Co., Ltd. (China), and directly used without further purification. H_2SO_4 (95–98%), $K_2S_2O_8$ (99%), and P_2O_5 (98%) were purchased from Sinopharm Chemical Reagent Co., Ltd. (China). High-purity (99.9%) graphite (325 mesh) was purchased from Qingdao Huatai Tech. Co., Ltd. (China), and was used to prepare the GO. NS with a 0.9% consistency and high-purity DW were also used in our study.

Fabrication of the GO/UHMWPE Composites

GO was prepared from high-purity graphite according to the modified method described by Hummers and Offeman.[20,31] In brief, graphite powder (3 g, 325 mesh) was put into a mixed solution that consisted of concentrated H_2SO_4 (12 mL), $K_2S_2O_8$ (2.5 g), and P_2O_5 (2.5 g); it was then kept at 80°C for 4.5 h with a hot plate. After that, the mixture was cooled to room temperature and diluted with DW (0.5 L) and left overnight. Then, the mixture was filtered and washed with DW by a 0.451-μm Millipore filter to remove the residual acid. The product was dried and was then subjected to oxidation by Hummers' method as follows: pretreated graphite powder was put into concentrated H_2SO_4 (120 mL and 0°C). Then, $KMnO_4$ (15 g) was added gradually under stirring below 20°C. Successively, the mixture was stirred at 35°C for 2 h and was then carefully diluted with 250 mL of H_2O. After that, the mixture was stirred for 2 h, and then, an additional 0.7 L of H_2O and 20 mL of 30% H_2O_2 were added. The resulting brilliant yellow mixture was filtered and washed with a 10 wt % HCl aqueous solution (1 L) to remove metal ions; this was followed by repeated washing with H_2O to remove the acid until the pH of the filtrate was neutral. The GO slurry was dried in a vacuum oven at 60°C and purified by dialysis for 1 week. Then the UHMWPE and its composites reinforced with GO were successfully fabricated with the steps of liquid-phase ultrasonic dispersion, high-speed ball-mill mixing, and hot-pressing molding technology with GO contents of 0.0, 0.1, 0.3, 0.7, and 1.0 wt % (weight percentage based on UHMWPE). The as-prepared powdery GO was first placed in a beaker (100 mL) containing 50 mL of ethanol solution. The solution was ultrasonically treated with an ultrasonic pole at 600 W for 0.5 h in an ice bath. The powdered UHMWPE (6 g) was added to the beaker and ultrasonically treated for 1 h with the same ultrasonic conditions. The resulting mixture was stirred at room temperature for 12 h and dried at 70°C in a vacuum oven for 24 h to remove the ethanol. The preliminary homogeneous GO/UHMWPE mixture underwent high-speed ball-mill mixing with a Pulverisette 7 (Fritsch, Germany) at 700 rpm for 2.5 h and dried at 70°C in a vacuum oven for another 24 h. According to Parasnis and Ramani[32] and Bankston et al.,[33] compression molding is a good processing route for UHMWPE because of its controllable morphological and high-quality product. Therefore, a dried homogeneous mixture of GO/UHMWPE was treated by hot compression molding with a DY-30 electric tablet press machine (180 W, 220 V, 50 Hz, Tianjin Keqi High & New Technology Corp.) at 195°C and 10 MPa for 30 min to form a rectangular slice with a size of $70 \times 70 \times 1$ mm^3. The temperature and compaction pressure chosen here corresponded to the optimum conditions reported by Tai et al.[20] The compaction time was considered to be sufficient for a uniform temperature profile to develop within the compacted powders. Before the wear tests, the specimens were cut into $30 \times 15 \times 1$ mm^3 pieces and cleaned with ethanol in an ultrasonic cleaner.

Characterization

The microstructure and microhardness of the GO/UHMWPE composites were examined with a high-resolution scanning electron microscope (HR-SEM; JSM-6701) and hardness testing machine (MH-5-VM, Shanghai Hengyi Precision Instrument Co., Ltd.), respectively. At least 15 points were measured by a permanent load of 10 g to obtain accurate average values of the microhardness of these samples. According to the research of Kumar, Piconi, and coworkers,[34–37] zirconia ceramic, as a joint prosthesis implant material, may have some advantages, including a low friction coefficient, no harmful effects to the human body, and a high strength and toughness. Therefore, in the DW

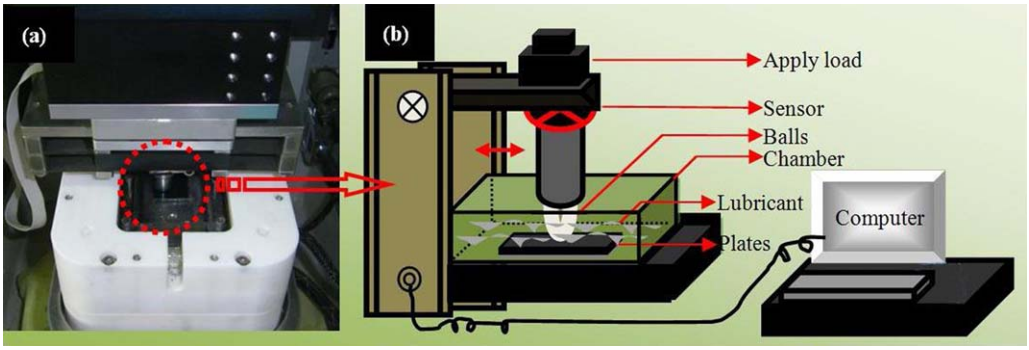

Figure 1. (a) Experimental setup and (b) schematic diagram of the ball-slide-on-plate wear test apparatus. [Color figure can be viewed in the online issue, which is available at wileyonlinelibrary.com.]

and NS lubrication conditions, the friction and wear properties of the composite samples were investigated in the joint simulator of an improved UMT-3MT tribometer apparatus (Universal Micro Tribometer, CETR; Figure 1) by sliding against ZrO_2 balls (Moh's hardness = 7.0 Pa, roughness = 0.03 μm, and diameter- = 4.0 mm).

The ball-on-disc UMT-3MT tribometer [Figure 1(a)] was used to evaluate the properties of the GO/UHMWPE composites.[37,38] The zirconia ceramic ball was fixed on the load arm, and the sample plates were fixed and submerged at the bottom of the chamber that contains the lubricating fluid [Figure 1(b)]. The chamber and sample plates were then rotated by an electrical motor controlled by a frequency converter. At the start of each wear test, pure DW or a 0.9% NS solution was introduced as the lubricant. The composites and ZrO_2 balls were ultrasonically cleaned with acetone before each test. A new ball or a new position of the ball was used for each friction test. Each wear test was repeated at least three times. To compare the samples, the applied normal load (N), the testing time, the sliding speed, the frequency, and the actual contact pressure between the balls and the composites were 5.0 N, 1 h, 10 mm/s, 3 Hz, and 6.56 MPa (calculated with the Hertzian contact model[4,39]), respectively. In the experimental apparatus, the strain gauge of the sensor was used to measure the frictional force on time, and the COF was calculated as follows:[20,34]

$$\mu = F/N$$

where μ is the specific coefficient of friction, F is the friction force (N), and N is the applied normal load (N). After the test, the WR was evaluated with a micro-XAM three-dimensional (3D) surface profiler and was calculated as follows:[13,20,34,39,40]

$$K\left(\mathrm{mm}^3\mathrm{N}^{-1}\mathrm{m}^{-1}\right) = \Delta V/(L \times N)$$

where K is the wear rate, ΔV is the wear volume (mm^3), and L is the sliding distance (m). In addition, all of the data values were determined with SPSS (Version 16.0), and the changes were analyzed with one-way analysis of variance (ANOVA) test for each group comparison among five levels of different GO contents.[20,41,42] Then, a two-way ANOVA and Tukey multiple-comparisons *post hoc* analysis were used to examine the effects and interaction of the reinforcement GO level and fabrication method on the measured microhardness of the composites and the effects and interaction of the reinforcement GO level and lubricant on the measured WR and scratch depth of the composites in different lubrication conditions (Table I). Significance level (p) values of less than 0.05 indicated that there were statistically significant differences in the group comparison. The correlation between the GO level and WR was studied with the correlation coefficient calculated by Origin 8.0, and the correlation simple linear regression equation was made as follows (Table II):

$$Y = A + B \times X$$

where A is a constant, B is the slope, X is the value of the independent variable, and Y is the value of the dependent variable. $B = 0$ and $B \neq 0$ indicate that the slope of the regression line is equal to zero and not equal to zero, respectively. If there is a significant linear relationship between X and Y, the slope will not equal zero. The p value was also chosen to be equal to 0.05. Finally, the morphologies of the worn surfaces of these composites and the balls were examined by a JSM-5600LV scanning electron microscope. The X-ray photoelectron (ESCALAB 210) spectrum was detected with Mg Kα as the excitation source with a radiation of 1253.6 eV to determine the element species on the ball surface.

Table I. Results of the Two-Way ANOVA for the Effects of the GO Content and the Fabrication Method on the Measured Microhardness and the Effects of the GO Content and the Lubricant on the Measured WR

	p				
Measurement	GO (wt %)	Fabrication method	Lubricant	GO (wt %) × Fabrication method	GO (wt %) × Lubricant
Microhardness (Hv)	<0.001	0.446		0.853	
WR (mm^3/Nm)	<0.001		0.001		0.917

Table II. Results of the WR Correlation Coefficient (R) Under the Lubrication Conditions of the DW and NS Solutions After Linear Fitting

		Linear regression for the data: $Y = A + B \times X$					
Parameter		Value ($\times 10^{-5}$)	Error ($\times 10^{-5}$)	R	SD ($\times 10^{-7}$)	N	p
In DW	A	1.8815	0.0123	−0.9977	1.1769	5	0.0001
	B	−0.0938	0.0037				
In NS	A	2.0048	0.0281	−0.9880	2.6835	5	0.0016
	B	−0.0942	0.0085				

SD = standard deviation.

RESULTS AND DISCUSSION

Microstructure of the GO/UHMWPE Composites

The cryogenic fracture surfaces of the pure UHMWPE and its composites were characterized by HR-SEM to evaluate the influence of GO in the composites. The fracture surfaces on the scanning electron microscopy (SEM) images of the composites with different GO contents are illustrated in Figure 2. For the pure UHMWPE, the fracture surface was relatively flat and demonstrated typical brittle fracture characteristics [Figure 2(a,b)]. After the crack was initiated, it rapidly propagated from one point to another. Additional cracks merged and expanded, and this resulted in the formation of riverlike patterns.[20,43] However, GO was embedded in the polymer upon addition [Figure 2(c–j)], and this resulted in the tight combination of the GO and the polymer. In the brittle fracture process, the GO sheets protruded and formed typical fractures on the surface of the graphene–polymer composites. Hence, the propagation of the crack was restrained and hampered.[44,45] In addition, when the GO content was increased, the fracture surface became coarser, and the morphology changed because of the protruding GO sheets. Similar features were also observed in other composites.[20,43–46]

Microhardness of the GO/UHMWPE Composites

The variations in the microhardness values of the GO/UHMWPE composites with increasing GO content are depicted in Figure 3 and Table III. All of the composites were successfully fabricated through the steps of liquid-phase ultrasonication dispersion, high-speed ball-mill mixing, and hot-pressing molding technology [Figure 3(b) and Table III through ball mixing] instead of the synthetic method with an optimized toluene-assisted mixing followed by hot pressing [Figure 3(a) and Table III through toluene mixing].[20] Significant differences were found in the mean microhardnesses among different levels of GO contents for each fabricated method except for the 0.1 and 0.3 wt % groups through high-speed ball-mill mixing/molding technology and the 0.1, 0.3, and 0.7 wt % groups with toluene-assisted mixing[20] (one-way ANOVA, $p < 0.05$; Table III and Figure 3). The two-way ANOVA showed a statistically significant effect of the reinforcement level of the GO content on the microhardness of the composites (two-way ANOVA, $p < 0.005$; Table I). However, the effect of the fabrication method was no statistically significant differences for the mean microhardness of the composites, and the interaction between the fabricated method and the reinforcement level was not statistically significant either (two-way ANOVA, $p > 0.05$; Table I). Compared with the pure UHMWPE, when the GO content was up to 1.0 wt %, the microhardness was increased by 13.80% through the high-speed ball-mill mixing/molding technology [Figure 3(b)]. This condition was due to the well-distributed GO sheets, which could bear the partial load and was essential for load transfer. Therefore, the microhardness of the GO/UHMWPE composites increased with the addition of GO.

Characterization of the Friction Behavior of the Specimens

The wear properties of the composite materials were primarily characterized by COF and WR.[39] The variations in the COF values of the GO/UHMWPE composites according to the wear

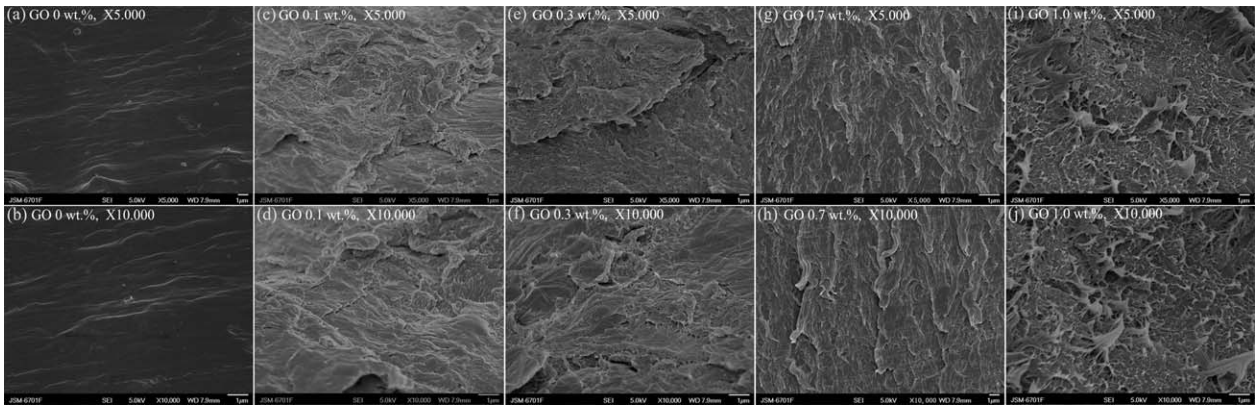

Figure 2. SEM images of the fracture surface of the GO/UHMWPE composites with the GO content: (a,b) 0, (c,d) 0.1, (e,f) 0.3, (g,h) 0.7, and (i,j) 1 wt % at different magnifications.

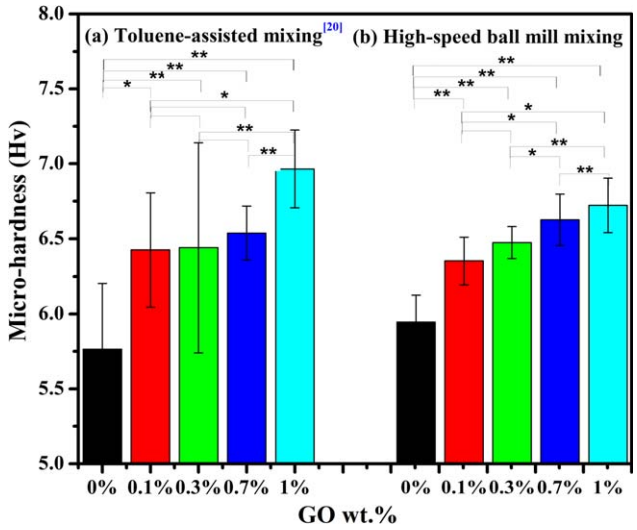

Figure 3. Variations in the microhardness values of the GO/UHMWPE composites with increasing GO content. The composites were successfully fabricated with (a) toluene-assisted mixing followed by hot pressing[20] and (b) liquid-phase ultrasonication dispersion, high-speed ball-mill mixing, and hot-pressing molding technology ($^{*}p < 0.05$, $^{**}p < 0.01$). [Color figure can be viewed in the online issue, which is available at wileyonlinelibrary.com.]

testing sliding time against the ZrO_2 ceramic ball in DW and NS lubricant conditions are demonstrated in Figure 4. After one run of wear testing, all of the COF values of the samples constantly decreased until they reached a plateau below the initial values [Figure 4(a,c)]. The same trend was observed in the results obtained from the polymer/metal couple.[39] Furthermore, during the steady-state period in each test, the average value of the COF (during 1500–3600 s) for the pure UHMWPE was approximately 0.056 in both DW [Figure 4(b)] and NS [Figure 4(d)] lubricant conditions. This result was in accordance with the results obtained in a previous report on pure UHMWPE sliding against ZrO_2 ceramic, which was approximately equal to $0.06 \pm 3\%$.[34] Furthermore, when the GO content was increased, the average values of COF of the composite in the two lubricant conditions did not significantly increase [Figure 4(b,d)]. All of the excellent friction properties of the GO/UHMWPE composites may have possibly been due to its small diameter, thin laminated structure, and superior self-lubricating properties of the GO sheet; this could have easily reduced the shear force and played a very important role in maintaining a low friction in the whole test process.

Characterization of the Wear Behavior of the Specimens

The effect of GO on the WR of the composite specimens sliding against ZrO_2 ceramic balls in DW and NS lubricant conditions are illustrated in Figure 5 and Table III. The WR of pure UHMWPE was the highest in both DW and NS lubricating conditions. The WR of these composites decreased remarkably as the GO content was increased. Significant differences were found in the mean WRs among different levels of GO content for each of the lubrication conditions, except for 0.3 and 0.7 wt % groups in DW and the 0.1 and 0.3 wt % groups in NS (one-way ANOVA, $p < 0.05$; Table III and Figure 5). The two-way ANOVA showed that not only the effect of GO content levels but also the lubrication conditions showed statistically significant differences for the mean WRs of the composites (two-way ANOVA, $p < 0.05$; Table I), but the interaction between the GO content levels and the lubrication conditions was not statistically significant (two-way ANOVA, $p > 0.05$; Table I). When the GO content reached 1.0 wt %, the WRs were decreased by 19.88 and 21.13% compared with the pure UHMWPE in the DW and NS lubricating conditions, respectively (Figure 5). The variation tendency and the correlation coefficients of the WRs of these composites were about -0.998 and -0.988 in the two lubrication conditions, respectively ($p < 0.05$; Figure 5 and Table II). Furthermore, it might have been related to the corrosion effect in NS that a much higher WR was found in the lubrication condition of NS than in those of DW.[47–51] The damage caused by friction decreased because the stress was effectively transferred by the inorganic filler of GO, which was uniformly distributed in the UHMWPE matrix.[20] Thus, the addition of GO evidently enhanced the wear resistance of UHMEPE at a low loading in the DW and NS lubricating conditions. Similar results were also observed in carbon nanotube (CNT)/UHMWPE,[15] CNT/polytetrafluoroethylene[52] and carbon nanofiber/UHMWPE composites,[53] in which the WR also decreased as the CNT or carbon nanofiber content increased.

Scratch Depths of the GO/UHMWPE Composites

The 3D morphology and its matching depths in the GO/UHMWPE composites are demonstrated in Figure 6. To calculate the scratch depth, the curvature of the surface was taken into account by approximation of the surface by a polynomial in a smooth solid line and then its integration to obtain the average value depths of the scratches, as shown in Figure 6(a).[54,55] For the pure UHMWPE [Figure 6(a,f) in DW and NS lubricating conditions, the depths of the scratches were about

Table III. Microhardness and WR Values of UHMWPE Reinforced with Different Concentrations of GO

	Microhardness (Hv)		WR ($mm^3/Nm \times 10^{-5}$)	
GO (wt %)	Toluene mixing[20]	Ball mixing	DW	NS
0.00	5.765 ± 0.44	6.01231 ± 0.19	1.796 ± 0.056	1.898 ± 0.046
0.10	6.426 ± 0.380	6.44231 ± 0.167	1.691 ± 0.035	1.806 ± 0.043
0.030	6.44 ± 0.7	6.57154 ± 0.113	1.583 ± 0.043	1.759 ± 0.053
0.70	6.537 ± 0.18	6.73231 ± 0.182	1.521 ± 0.023	1.636 ± 0.044
1.00	6.965 ± 0.26	6.83462 ± 0.193	1.417 ± 0.027	1.512 ± 0.047

Means and standard deviations are shown for each group.

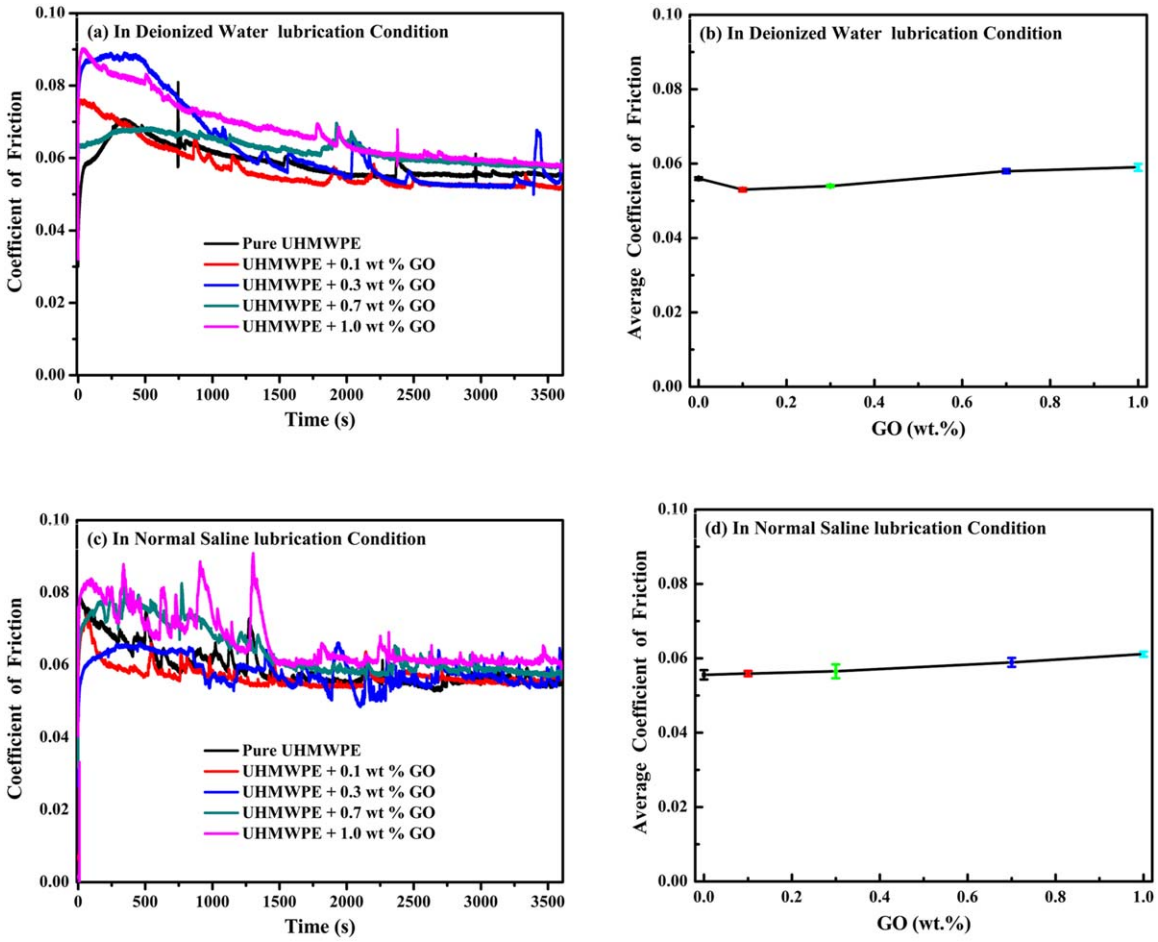

Figure 4. Variations in the COF values of the GO/UHMWPE composites according to the wear sliding time against the ZrO_2 ceramic ball under (a) DW and (b) NS lubrication conditions. The vignettes stand for the average value of the COF in a stable period during wear testing. [Color figure can be viewed in the online issue, which is available at wileyonlinelibrary.com.]

−5.19 and −5.89 μm in DW and NS, respectively. In addition, as the GO content increased in the GO/UHMWPE composites, the depths of the scratches became much shallower in the two lubricant conditions. When the GO content was up to 1.0 wt %, the depths of the scratches were decreased by 22.93 and 23.77% in the DW and NS lubricating conditions, respectively (Figure 6). Thus, we inferred that much less wear loss could be found in the DW lubricating condition than in the NS condition because of the corrosive influence of chlorine ions in the NS.[28,48] Therefore, it also indicated that with increasing GO content in the GO/UHMWPE composites, the scratch depths of these composites could significantly decrease, and the wear resistance performance could significantly improve in these two lubricating conditions.

Worn Surface Topographies of the GO/UHMWPE Composites

The worn surface of the GO/UHMWPE composites were sputtered with a gold coating to render them as electrical conductors before the examinations of their topographies with SEM. SEM images of the worn surfaces of the GO/UHMWPE composites and the contact surface of the ZrO_2 ceramic balls are shown in Figure 7. For pure UHMWPE [Figure 7(a,k) in the DW and NS lubricating conditions, respectively], the worn sur-

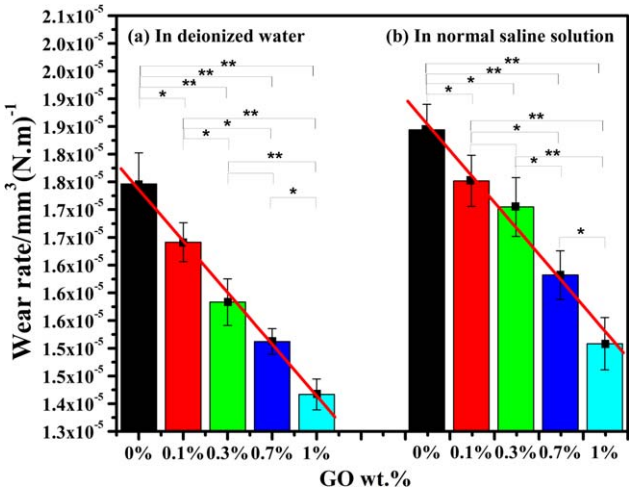

Figure 5. Variations in the WR of the GO/UHMWPE composites according to the different GO contents sliding against the ZrO_2 ceramic ball in DW and NS lubrication conditions. The discrepancy was the standard deviation ($^*p < 0.05$, $^{**}p < 0.01$). [Color figure can be viewed in the online issue, which is available at wileyonlinelibrary.com.]

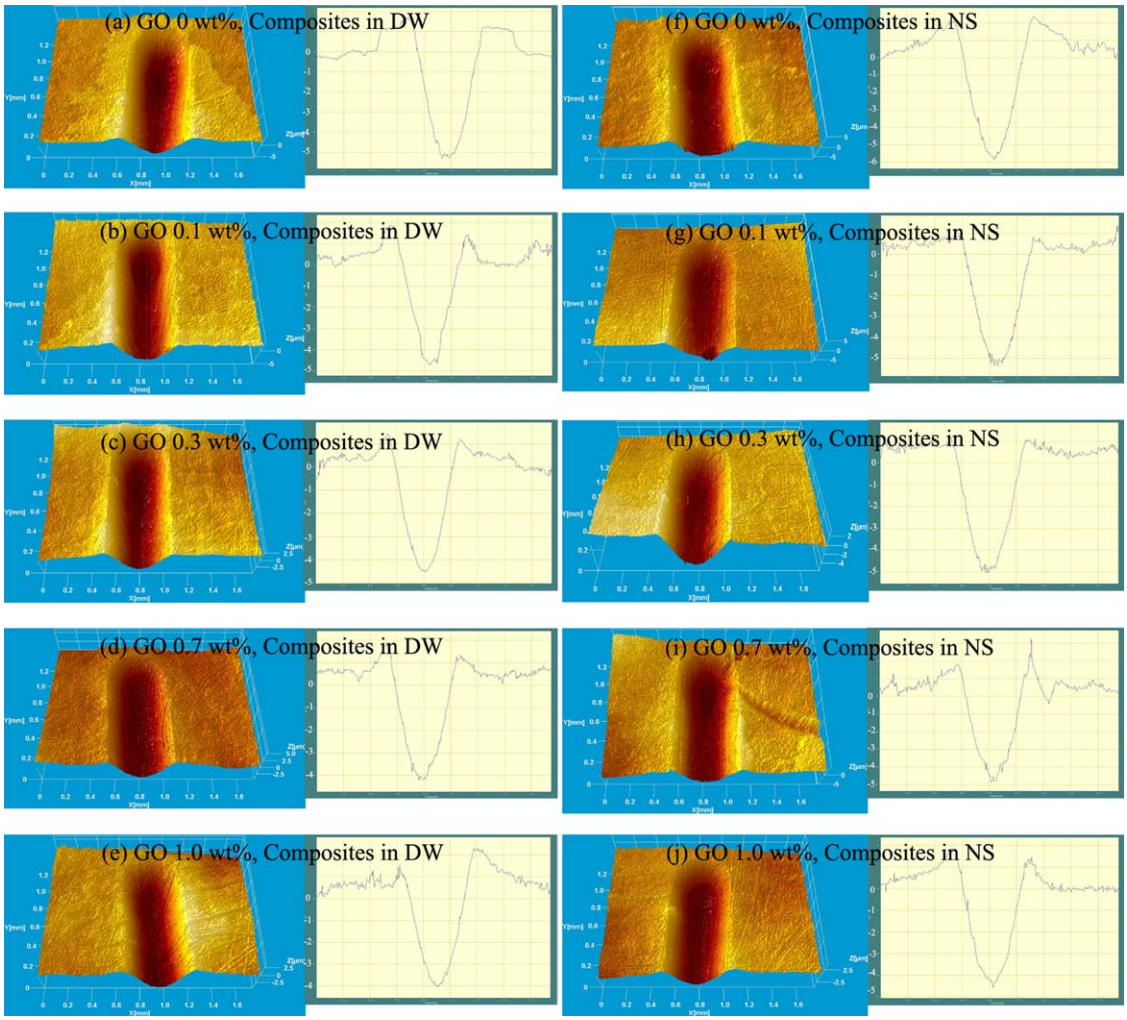

Figure 6. Typical 3D morphology and its matching depths of the GO/UHMWPE composites after the wear test in (a–e) DW and (f–j) NS. The GO contents were (a,f) 0.0, (b,g) 0.1, (c,h) 0.3, (d,i) 0.7, and (e,j) 1.0 wt %. [Color figure can be viewed in the online issue, which is available at wileyonlinelibrary.com.]

face had microcracks, deep grooves, and serious fatigue-separated layers after they slid against the ZrO_2 balls in the DW and NS lubricating conditions.[20,56] When GO was added and as the GO content was increased in the GO/UHMWPE composites, the damage of the worn surfaces and the scratches on the GO/UHMWPE composite plate not only became smoother but also became shallower in the DW and NS lubricant conditions [Figure 7(a–e) and Figure 7(k–o), respectively]. These results indicate that it could significantly alter the mechanical properties and improve the wear resistance performance of UHMWPE with the addition of GO. The well-distributed and high-aspect-ratio GO sheets, which could bear a partial load and were essential for the load transfer in the GO/UHMWPE composites, provided a large surface area to facilitate the interaction between the UHMWPE and GO. As a result, the shear force was effectively transferred from the matrix to the reinforcement.[45] Therefore, the wear resistance of these composites could be significantly improved. All of these results were also in accordance with the low WR value obtained when GO was used to enhance the wear resistance of the polymers at low loadings in dry and water-lubricating conditions.[20,57]

X-ray Photoelectron Spectroscopy (XPS) Analysis of the ZrO_2 Ceramic Balls

The XPS results of the ZrO_2 ceramic balls after the wear test are shown in Figure 8(a). After curve-fitting, the peak of the C_{1s} electrons at 284.50 eV, shown in Figure 8(b,c), corresponded with the C—C and C—H bonds of the UHMWPE in both the DW and NS lubricating conditions.[58–61] The small peaks from 286.00 to 289.00 eV (those at 286.65, 287.70, and 289.00 eV corresponded to the C—O, C═O, and O—C═O groups, respectively) indicated the formation of surface photooxidation products caused by air.[62] Moreover, the spectra showed that the film contained oxygen in addition to carbon. As shown in Figure 8(d,e), the surface compositions of the O_{1s} bands appearing at 529.60, 532.20, 531.20, and 533.40 eV corresponded to the O═C—O—H, C═O, and O—C═O groups in the DW and NS lubricating conditions, respectively. The appearance of the O_{1s}

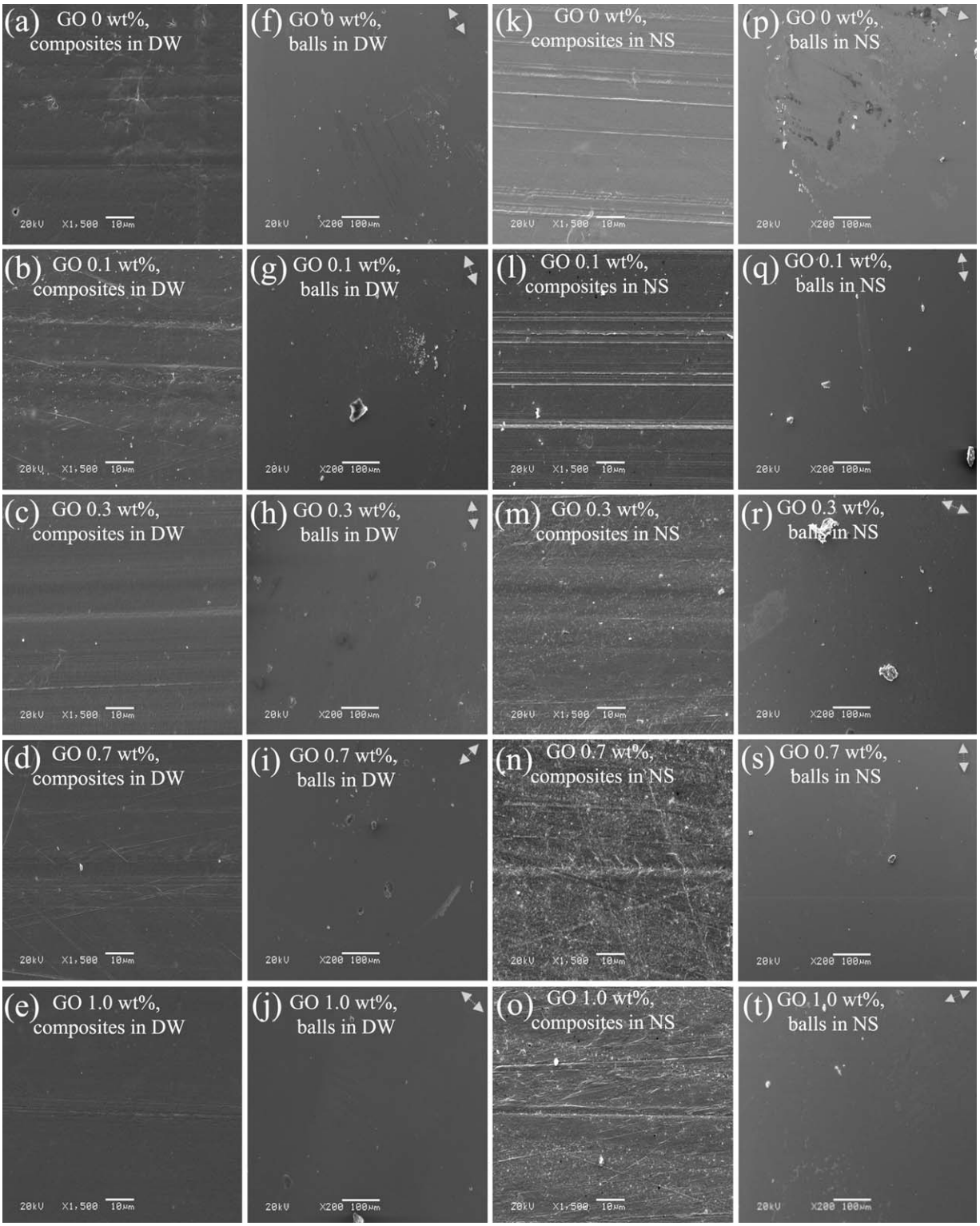

Figure 7. SEM images of the (a–e,k–o) pure UHMWPE and GO/UHMWPE composites and (f–j,p–t) ZrO_2 ceramic balls pairs after the tribological tests in (a–j) DW and (k–t) NS. The GO contents were (a,k) 0.0, (b,l) 0.1, (c,m) 0.3, (d,n) 0.7, and (e,o) 1.0 wt %. The double-headed arrows indicate the sliding direction.

peak may have been from the oxygen adsorption, polymers, and H_2O (Binding energy (BE) = 533.40 eV) when the sample was exposed to the atmosphere.[61,63] These chemical species, which are produced from the friction, heat, and chemical reactions between the composites and balls in the friction process, might have had a very important effect on the friction and wear properties of the materials.[53,64] These effects included a decrease in WR and the improvement in the wear resistance of the GO/

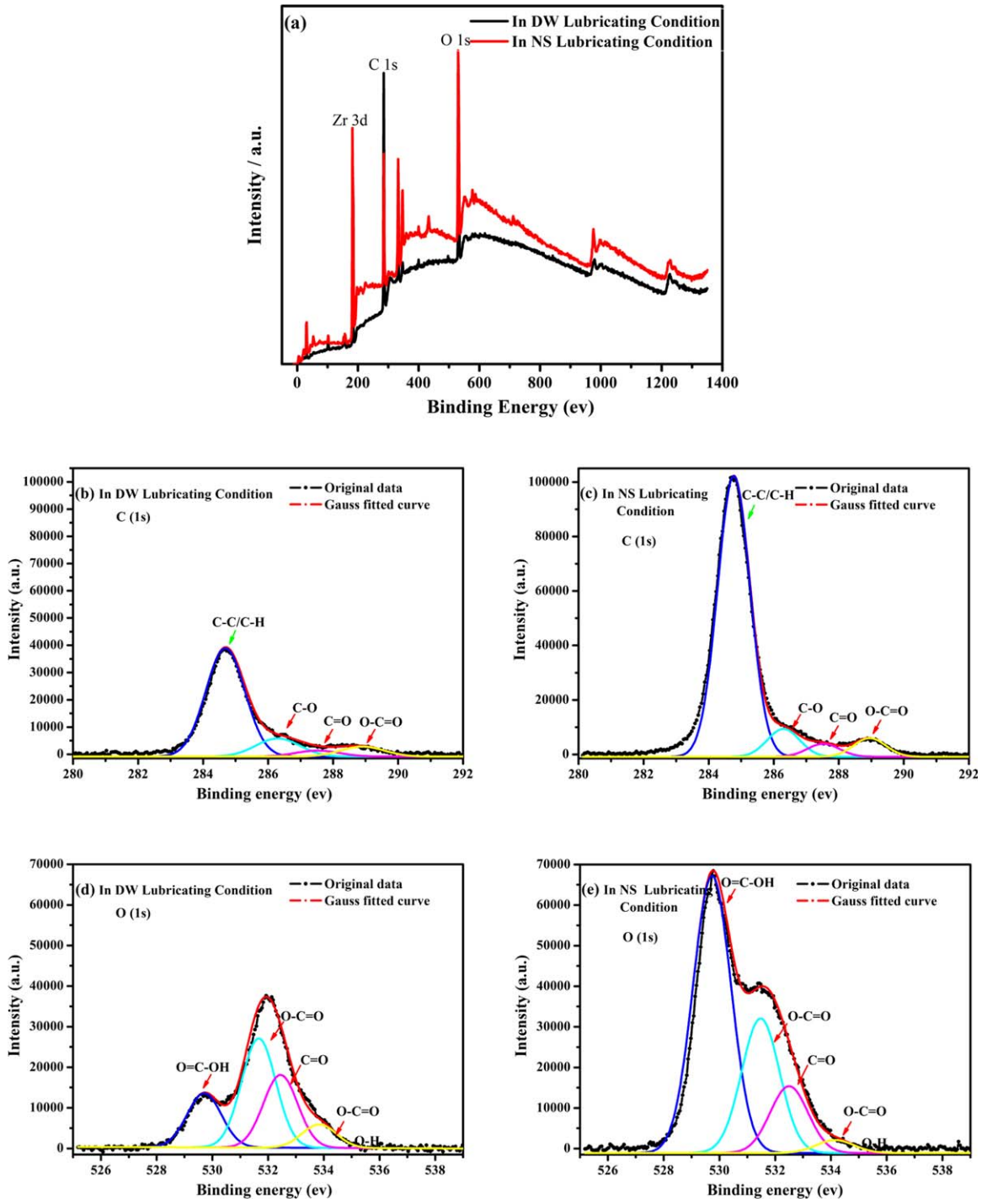

Figure 8. (a) XPS results from the surface of the balls after wear testing in DW and NS lubricating conditions. The curve-fitting for the peaks of C_{1s} in (b) DW and (c) NS and O_{1s} peaks in (d) DW and (e) NS. [Color figure can be viewed in the online issue, which is available at wileyonlinelibrary.com.]

UHMWPE composites in the DW and NS lubrication conditions.

CONCLUSIONS

GO, as an inorganic filler, was effectively dispersed in UHMWPE through the steps of liquid-phase ultrasonication dispersion, high-speed ball-mill mixing, and hot-pressing molding technology. In both the DW and NS lubricating conditions and compared with the pure UHMWPE, both the microhardness and wear resistance of the GO/UHMWPE composites gradually increased, and the COF slightly increased. The wear mechanism of the pure UHMWPE was mainly controlled by a slight fatigue wear at a low *F*. After the addition of GO, the wear mechanism of the GO/UHMWPE composites transformed from fatigue wear to abrasive wear because of the contribution

of the GO sheets at a low *F*. The wear resistances of the composites significantly improved because of the well-distributed GO sheets, which could bear a partial load and were essential for load transfer. Furthermore, the tribological properties in the other lubricants of a physiological synovial fluid, such as bovine serum and hyaluronic acid, among others, will be considered in our future work for verification to obtain a better understanding of the friction and wear behaviors of these composites.

ACKNOWLEDGMENTS

The authors are grateful for financial support from the National Natural Science Foundation of China (contract grant number 51005225) and the Top Hundred Talents Program of the Chinese Academy of Sciences.

REFERENCES

1. Krzypow, D. J.; Rimnac, C. M. *Biomaterials* **2000**, *21*, 2081.
2. Xiong, D. S.; Gao, Z.; Jin, Z. M. *Surf. Coat. Technol.* **2007**, *201*, 6847.
3. Ohta, M.; Hyon, S. H.; Tsutumi, S. *Wear* **2003**, *255*, 1045.
4. Chen, Y. F.; Qi, Y. Y.; Tai, Z. X.; Yan, X. B.; Zhu, F. L.; Xue, Q. *J. Eur. Polym. J.* **2012**, *48*, 1026.
5. Weimin, F.; Qing, W.; Songnian, T. *Chin. J. Orthop.* **1998**, *18*, 518.
6. Harris, W. H. *Clin. Orthop. Relat. Res.* **1995**, *311*, 46.
7. Wang, Q. L.; Liu, J. L.; Ge, S. R. *J. Bionic Eng.* **2009**, *6*, 378.
8. Wang, Q.; Zhang, D.; Ge, S. *J. Eng. Tribol.* **2007**, *221*, 307.
9. Hashimoto, M.; Takadama, H.; Mizuno, M.; Yasutomi, Y.; Kokubo, T. *Key Eng. Mater.* **2002**, *240*, 415.
10. Xiong, D. S.; Lin, J. M.; Fan, D. L.; Jin, Z. M. *J. Mater. Sci.: Mater. Med.* **2007**, *18*, 2131.
11. Xie, X. L.; Tang, C. Y.; Chan, K. Y. Y.; Wu, X. C.; Tsui, C. P.; Cheung, C. Y. *Biomaterials* **2003**, *24*, 1889.
12. Roy, S.; Pal, S. *Bull. Mater. Sci.* **2002**, *25*, 609.
13. Park, H. J.; Kwak, S. Y.; Kwak, S. *Macromol. Chem. Phys.* **2005**, *206*, 945.
14. Wood, W. J.; Maguire, R. G.; Zhong, W. H. *Compos. B.* **2011**, *42*, 584.
15. Zoo, Y. S.; An, J. W.; Lim, D. P.; Lim, D. S. *Tribol. Lett.* **2004**, *16*, 305.
16. Samad, M. A.; Sinha, S. K. *Wear* **2011**, *270*, 395.
17. Tetik, R. D.; Galante, J. O.; Rostoker, W. *J. Biomed. Mater. Res.* **1974**, *8*, 231.
18. Delgado-Rangel, J. A.; Addiego, F.; Eddoumy, F.; Ahzi, S.; Patlazhan, S.; Toniazzo, V.; Ruch, D. *J. Appl. Polym. Sci.* **2012**, *125*, 4316.
19. Carotenuto, G.; Nicola, S. D.; Palomba, M.; Pullini, D.; Horsewell, A.; Hansen, T. W.; Nicolais, L. *Nanotechnology* **2012**, *23*, 485705.
20. Tai, Z. X.; Chen, Y. F.; An, Y. F.; Yan, X. B.; Xue, Q. *J. Tribol. Lett.* **2012**, *46*, 55.
21. Donald, J. M.; Hooper, K.; Hopenhayn-Rich, C. *Environ. Health Perspect.* **1991**, *94*, 237.
22. Neubert, D.; Bochert, G.; Gericke, C.; Hanke, B.; Beckmann, G. *Toxicology* **2001**, *168*, 139.
23. Ebramzadeh, E.; Sangiorgio, S. N.; Lattuada, F.; Kang, J. S.; Chiesa, R.; McKellop, H. A.; Dorr, L. D. *J. Bone Joint Surg.* **2003**, *85*, 2378.
24. Shanbhag, A. S.; Bailey, H. O.; Hwang, D. S.; Cha, C. W.; Eror, N. G.; Rubash, H. E. *J. Biomed. Mater. Res.* **2000**, *53*, 100.
25. Kobayashi, A.; Bonfield, W.; Kadoya, Y.; Yamac, T.; Freeman, M. A. R.; Scott, G.; Revell, P. A. *J. Eng. Med.* **1997**, *211*, 11.
26. Ralphs, J. R.; Benjamin, M. *J. Anat.* **1994**, *184*, 503.
27. Sawae, Y.; Yamamoto, A.; Murakami, T. *Tribol. Int.* **2008**, *41*, 648.
28. Xiong, D. S.; Ge, S. R. *Wear* **2001**, *250*, 242.
29. Cho, H. J.; Wei, W. J.; Kao, H. C.; Cheng, C. K. *Mater. Chem. Phys.* **2004**, *88*, 9.
30. Liu, C. Z.; Wu, J. Q.; Li, J. Q.; Ren, L. Q.; Tong, J.; Arnell, A. D. *Wear* **2006**, *260*, 109.
31. Hummers, W. S.; Offeman, R. E. *J. Am. Chem. Soc.* **1958**, *80*, 1339.
32. Parasnis, N. C.; Ramani, K. *J. Mater. Sci.: Mater. Med.* **1998**, *9*, 165.
33. Bankston, B. A.; Keating, M. E.; Ranawat, C.; Faris, P. M.; Ritter, M. A. *Clin. Orthop. Relat. Res.* **1995**, *317*, 37.
34. Kumar, P.; Oka, M.; Ikeuchi, K.; Shimizu, K.; Yamamuro, T.; Okumura, H.; Kotoura, Y. *J. Biomed. Mater. Res.* **1991**, *25*, 813.
35. Piconi, C.; Maccauro, G. *Biomaterials* **1999**, *20*, 1.
36. Keegan, G. M.; Learmonth, I. D.; Case, C. *J. Bone Joint Surg. Br.* **2007**, *89*, 567.
37. Platon, F.; Fournier, P.; Rouxel, S. *Wear* **2001**, *250*, 227.
38. Ge, S. R.; Wang, Q. L.; Zhang, D. K.; Zhu, H.; Xiong, D. S.; Huang, C. H.; Huang, X. L. *Wear* **2003**, *255*, 1069.
39. Geringer, J.; Tatkiewicz, W.; Rouchouse, G. *Wear* **2011**, *271*, 2793.
40. Xiong, D. S.; Jin, Z. M. *Surf. Coat Technol.* **2004**, *182*, 149.
41. Kim, D. W.; Lee, K. Y.; Jun, Y.; Lee, S. J.; Park, C. K. *Int. J. Precis. Eng. Manuf.* **2011**, *12*, 1111.
42. Converse, G. L.; Yue, W. M.; Roeder, R. K. *Biomaterials* **2007**, *28*, 927.
43. Qiu, J. J.; Wang, S. R. *J. Appl. Polym. Sci.* **2011**, *119*, 3670.
44. Ramanathan, T.; Abdala, A. A.; Stankovich, S.; Dikin, D. A.; Herrera-Alonso, M.; Piner, R. D.; Adamson, D. H.; Schniepp, H. C.; Chen, X.; Ruoff, R. S. *Nat. Nanotechnol.* **2008**, *3*, 327.
45. Rafiee, M. A.; Rafiee, J.; Wang, Z.; Song, H.; Yu, Z. Z.; Koratkar, N. *ACS Nano* **2009**, *3*, 3884.
46. Lahiri, D.; Dua, R.; Zhang, C.; Socarraz-Novoa, I.; Bhat, A.; Ramaswamy, S.; Agarwal, A. *ACS Appl. Mater. Interfaces* **2012**, *4*, 2234.
47. Waters, E. P. J.; Spedding, P. L.; Dohert, A. P.; Spedding, R. L. *Asia-Pac. J. Chem. Eng.* **2009**, *4*, 80.
48. Wang, J. Z.; Yan, F. Y.; Xue, Q. *J. Tribol. Lett.* **2009**, *35*, 85.

49. Tsukamoto, R.; Chen, S.; Asano, T.; Ogino, M.; Shoji, H.; Nakamura, T.; Clarke, I. C. *Acta Orthop.* **2006**, *77*, 505.
50. Kim, D. W.; Lee, K. Y.; Jun, Y.; Lee, S. J.; Park, C. K. *Int. J. Precis. Eng. Manuf.* **2011**, *12*, 1111.
51. Puska, M. A.; Lassila, L. V.; Närhi, T. O.; Yli-Urpo, A. U. O.; Vallittu, P. K. *Appl. Compos. Mater.* **2004**, *11*, 17.
52. Chen, W. X.; Li, F.; Han, G.; Xia, J. B.; Wang, L. Y.; Tu, J. P.; Xu, Z. D. *Tribol. Lett.* **2003**, *15*, 275.
53. Xiong, D. S. *Mater. Lett.* **2005**, *59*, 175.
54. Xu, S.; Akchurin, A.; Liu, T.; Wood, W.; Tangpong, X. W.; Akhatov, I. S.; Zhong, W. H. *J. Tribol.* **2012**, *134*, 041602.
55. Pettarin, V.; Churruca, M. J.; Felhös, D.; Karger-Kocsis, J.; Frontini, P. M. *Wear* **2010**, *269*, 31.
56. Liu, H. J.; Pei, Y. N.; Xie, D.; Deng, X. R.; Leng, Y. X.; Jin, Y.; Huang, N. *Appl. Surf. Sci.* **2010**, *256*, 3941.
57. Li, Y. Q.; Wang, Q. H.; Wang, T. M.; Pan, G. Q. *J. Mater. Sci.* **2011**, *47*, 730.
58. Liu, H. J.; Xie, D.; Qian, L. M.; Deng, X. R.; Leng, Y. X.; Huang, N. *Surf. Coat Technol.* **2011**, *205*, 2697.
59. Samad, M. A.; Sinha, S. K. *Tribol. Int.* **2011**, *44*, 1932.
60. Ambrosio, L.; Carotenuto, G.; Marletta, G.; Nicolais, L.; Scandurra, A. *J. Mater. Sci.: Mater. Med.* **1996**, *7*, 723.
61. Yang, D.; Velamakanni, A.; Bozoklu, G.; Park, S.; Stoller, M.; Piner, R. D.; Stankovich, S.; Jung, I.; Field, D. A.; Ventrice, C. A. *Carbon* **2009**, *47*, 145.
62. Kwak, S.; Noh, D. I.; Chun, H. J.; Lim, Y. M.; Nho, Y. C.; Jang, J. W.; Shim, Y. B. *Macromol. Res.* **2009**, *17*, 603.
63. Xie, D.; Liu, H. J.; Deng, X. R.; Leng, Y. X.; Huang, N. *Appl. Surf. Sci.* **2009**, *256*, 284.
64. Sinha, S. K.; Lee, C. B.; Lim, S. C. *Tribol. Lett.* **2008**, *29*, 193.